physica status solidi c
www.pss-c.com
current topics in solid state physics

Probing the interaction between a single quantum dot and a photonic crystal cavity

Ilya Fushman[1,2], Dirk Englund[1,2], Andrei Faraon[1,2], and Jelena Vuckovic[1]

[1] Applied Physics, Stanford University, Stanford CA, 94305, USA
[2] These authors contributed equally

Received 12 October 2007, revised 2 January 2008, accepted 17 January 2008
Published online 17 June 2008

PACS 42.50.Dv, 42.50.Pq , 42.55.Tv, 42.70.Qs

This article reviews our recent work on the development of nanophotonic devices for quantum information processing. We have developed a temperature tuning technique, that allows us to independently tune photonic crystal cavities and quantum dots on the same chip. The high quality factor to mode volume ratio of such cavities leads to a strong interaction between the cavity and the quantum dot. The cavity modifies the quantum dot lifetime, which, in turn, modifies the transmission properties of the cavity. We observe that the resonant nonlinearity of the quantum dot is greatly enhanced by the recirculation of light, and leads to a giant optical nonlinearity, where single photons are able to saturate the quantum dot and modify the transmission function of the cavity. Along with these results, we review the experimental developments, which have led to the realization of the experiment.

phys. stat. sol. (c) **5**, No. 9, 2808–2815 (2008) / **DOI** 10.1002/pssc.200779289

phys. stat. sol. (c) **5**, No. 9, 2808–2815 (2008) / **DOI** 10.1002/pssc.200779289

physica status solidi c
www.pss-c.com
current topics in solid state physics

Probing the interaction between a single quantum dot and a photonic crystal cavity

Ilya Fushman[1,2], Dirk Englund[1,2], Andrei Faraon[1,2], and Jelena Vuckovic[1,*]

[1] Applied Physics, Stanford University, Stanford CA, 94305, USA
[2] These authors contributed equally

Received 12 October 2007, revised 2 January 2008, accepted 17 January 2008
Published online 17 June 2008

PACS 42.50.Dv, 42.50.Pq , 42.55.Tv, 42.70.Qs

* Corresponding author: e-mail jela@stanford.edu

This article reviews our recent work on the development of nanophotonic devices for quantum information processing. We have developed a temperature tuning technique, that allows us to independently tune photonic crystal cavities and quantum dots on the same chip. The high quality factor to mode volume ratio of such cavities leads to a strong interaction between the cavity and the quantum dot. The cavity modifies the quantum dot lifetime, which, in turn, modifies the transmission properties of the cavity. We observe that the resonant nonlinearity of the quantum dot is greatly enhanced by the recirculation of light, and leads to a giant optical nonlinearity, where single photons are able to saturate the quantum dot and modify the transmission function of the cavity. Along with these results, we review the experimental developments, which have led to the realization of the experiment.

1 Introduction Our goal is the development of architecture for on-chip quantum information processing devices. An attractive paradigm for a quantum information processing device is a network of stationary qubits that are connected by flying photonic qubits. The stationary nodes of such a system can be atoms with two stable ground states, or the spin states of electrons or nuclei. An optical cavity can be used to efficiently transfer information between the stationary qubit and the connecting photonic qubit and facilitate the interaction between the two. The states of the stationary qubits determine the routing of photonic information in such a network. Furthermore, interactions between several photonic qubits, and hence remote stationary qubits, can be facilitated by the stationary qubit inside the cavity [1,2]. Towards these ends, we have been developing photonic cavities, photonic networks, and the interaction between stationary qubits and photons in the Gallium Arsenide (GaAs) material system.

We have chosen GaAs due to the availability of Indium Arsenide (InAs) quantum dots with large dipole moments, and the well understood semiconductor processing techniques for the development of high quality factor (Q), small optical mode volume (V) photonic crystal (PC) cavities. This system has great potential for realizing a high density, monolithically integrated quantum optical network made up of cavity nodes connected by waveguides [3]. In the past few years, tremendous progress has been made in this particular subfield of quantum optics, with the development of efficient single photon sources [4], the demonstration of strong coupling between a quantum dot and PC cavity [5,6], and the generation and transfer of single photons on a PC chip [3]. The PC network architecture has the additional benefit of being potentially useful for commercial photonics applications, and therefore active research for these applications can be transferred to the quantum information processing domain. In Section 2, we review the design and fabrication methods for photonic crystal cavi-

ties used in our work. In Section 3 we review the theory of coupling between quantum dots and PC cavities in the strong and weak coupling regimes. We present our results on the development of single photon sources and control over the spontaneous emission rates of quantum dots in PC cavities [4]. In Section 4 we review the theory of resonant light scattering from quantum dots coupled to PC cavities, and present our novel local temperature tuning technique [7], which allows us to resonantly probe the quantum dot inside the PC cavity. We show that the dot strongly modifies the cavity spectrum, and acts as a saturable nonlinearity at powers corresponding to a single photon per cavity lifetime [8], and discuss the implications for coherent control on the photonic crystal chip.

2 Photonic crystal design and fabrication Our experiments are based on planar photonic crystal (PC) devices in GaAs with incorporated InAs quantum dots (QDs). QD wafers are grown by molecular beam epitaxy by our collaborators. They contain an active region consisting of a 150-160 nm thick GaAs layer with a centered InAs/GaAs QD layer. The active layer is grown on an AlGaAs sacrificial layer (with Al content of 80%), which is in turn grown on a GaAs substrate. The suspended PC structures are fabricated on such a wafer by a combination of electron beam lithography and dry etching (which creates a PC pattern in the top GaAs layer containing QDs), and a final wet etching step which removes a sacrificial layer underneath PC components. An example of fabricated GaAs PC cavities using the described procedure is shown in Fig. 1. In the same figure we also show the photoluminescence spectrum from the same type of cavity, obtained by exciting embedded InAs QDs, and indicating a cavity quality (Q) factor of 20000.

3 Interaction between coherent light and a quantum dot in a PC cavity: theory The theory of an emitter coupled to an optical cavity can be found in [9, 2]. The novelty of photonic crystal cavities is that the optical mode volume is very small (on the order of $(\lambda/n)^3$, where n is the refractive index of the material, and λ is the resonant wavelength of the cavity), and therefore even with moderate quality factors, highly nonlinear effects can occur in this system.

We consider the quantum dot to be a two level system with a long-lived ground state, and a dipole decay rate $\gamma/2\pi = 0.2$ GHz. InAs quantum dots at low temperature ($\approx 10-20$ K) are generally close to Fourier-limited, and so the dipole dephasing rate can be approximated to be one half of the dipole decay rate. The coupling of the quantum dot dipole to the cavity electric field is given by the Rabi frequency:

$$g = \frac{|\boldsymbol{\mu}|}{\hbar}\sqrt{\frac{\hbar\omega_d}{2\epsilon_M V}}\frac{E(\mathbf{r})}{|E(\mathbf{r}_M|}cos\left(\frac{\boldsymbol{\mu}\cdot\hat{e}}{|\mu|}\right) \qquad (1)$$

In this expression, $\mathbf{r}_M$ is the point where the cavity mode field $E(\mathbf{r})$ has a maximum, $\hat{e}$ is the unit vector along the direction of $E(\mathbf{r})$, ϵ_M is the dielectric constant at this point, $\boldsymbol{\mu}$ is the dot dipole moment, ω_d is the dot emission frequency, and V is the optical mode volume defined as $V = \frac{\int d^3\mathbf{r}\epsilon(\mathbf{r})|E(\mathbf{r})|^2}{\epsilon_M|E(\mathbf{r}_M)|^2} \approx 0.75\left(\frac{\lambda}{n}\right)^3$. Values of g clearly depend on position and dipole alignment, with the maximum dipole moment of $g_{max} \approx 300$ GHz in this system.

When a quantum dot is resonant with the PC cavity at frequency ω_c, the dot emission is modified. The degree of modification depends on the parameters g, γ and the field decay rate $\kappa = \omega_c/(2Q)$. In the frame rotating with the dot frequency, the eigenvalues of the cavity-dot system are:

$$\omega_\pm = i\frac{\omega_c+\omega_d}{2} - \left(\frac{\kappa+\gamma}{2}\right) \pm \sqrt{\left(\frac{\kappa-\gamma}{2}\right)^2 - g^2} \quad (2)$$

This equation can be taken to two limits, one in which the square root is real, and the other, in which it is imaginary. In the first case, the two eigenvalues are real and correspond to decay rates of the cavity and quantum dot. This regime is typically termed the weak coupling regime. In the case of an imaginary square root, the composite quantum dot system decays at one rate, and oscillates at two frequencies corresponding to the coherent exchange of photons between the dot and cavity.

3.1 Weak coupling regime For our system, $\kappa/2\pi \approx 16$GHz, The eigenvalues on the weak coupling regime can be found by expanding the square root in Eq. (2) for the case $\kappa >> g >> \gamma$ as:

$$\omega_+ = -\left(\gamma + \frac{g^2}{\kappa}\right) \approx -\frac{g^2}{\kappa} \qquad (3)$$

$$\omega_- \approx -\kappa \qquad (4)$$

In this case, ω_- corresponds to the cavity and ω_+ corresponds to the dot dipole. The dot excited state population decays with a rate $2\omega_+$ inside the cavity. As can be seen, the value of the dot decay is modified relative to the bulk value γ. The ratio of the lifetime in the cavity γ_c to that in the bulk $\gamma_c/\gamma = 2\omega_+/\gamma$ is dependent on position, dipole alignment and frequency detuning according to

$$\frac{\gamma_c}{\gamma} = \frac{3}{4\pi^2}\frac{Q}{V}\left(\frac{\lambda}{n}\right)^3 \qquad (5)$$

$$\times \left(\frac{E(\mathbf{r})}{E(\mathbf{r}_M)}\right)^2\left(\frac{\boldsymbol{\mu}\cdot\hat{e}}{|\boldsymbol{\mu}|}\right)^2 \frac{1}{1+4Q^2\left(\frac{\omega_c}{\omega_d}-1\right)^2} \qquad (6)$$

At the point of maximum spatial and frequency alignment, the ratio γ_c/γ reduces to the Purcell factor $F = \frac{3}{4\pi^2}\frac{Q}{V}\left(\frac{\lambda}{n}\right)^3$. The fraction of photons emitted into the single cavity mode is then $\beta = \frac{F}{f+F}$, where f accounts for the reduction in the available states inside the photonic bandgap material.

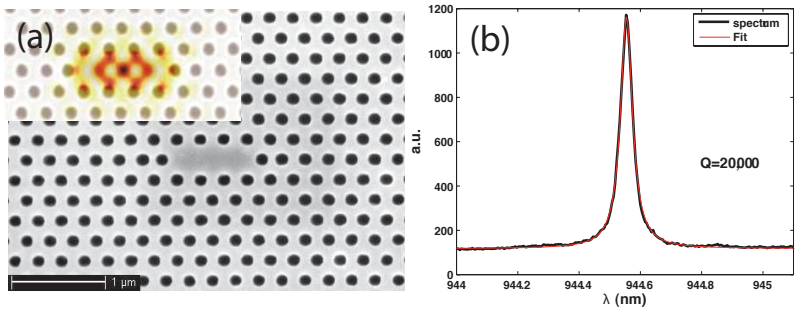

Figure 1 A scanning electron micrograph (SEM) of a fabricated L3 cavity is shown in (a). The inset shows the electric field amplitude, computed with Finite Difference Time Domain software, overlaid on the SEM image. (b) Shows a typical cavity spectrum illuminated by InAs quantum dots that are coupled to the cavity. A Q of 20,000 is inferred from the fit.

We now review our experiment, in which we have shown that the emission rate of dots can be both suppressed and enhanced by the interaction with the cavity [4]. Spatial and spectral alignment can result in up to ten-fold enhancement or almost ten-fold suppression of the dot radiative rate when compared to the bulk rate (Figs. 2 and 3), with a 100-fold enhancement being theoretically possible for the values of Q and V used in this experiment. In Fig. 2(a), the lifetimes of cavity coupled and quantum dots are derived from the time-dependent photoluminescence signal. Suppression and enhancement relative to the bulk lifetime of $\approx 1ns$ are observed. To show that the photonic bandgap also suppresses the emission rate, we show the rate for a quantum dot which is inside the cavity, but emitting at 90^o relative to the cavity polarization. One of the most important applications to quantum optics is the generation of fast, efficiently extracted and indistinguishable single photons. important applications for indistinguishable single photon sources. Figure 2 (b) and (c) show the autocorrelation function for quantum dots inside the PC cavity, which are both enhanced (b) and suppressed (c). Both show strong antibunching at zero time delay, indicating that these are good single photon sources. The larger width of peaks in (b) indicates that this dot is slowly emitting, as confirmed in (a). Our results indicate that spectral and spatial alignment have a great impact on dot radiative properties, and that spectral alignment can be used to control absorption and emission rates of InAs quantum dots in PC cavities. While spatial alignment is in our case probabilistic, other groups have made significant progress towards precise alignments of the dot position and dipole moment to the PC cavity [6].

3.2 Strong coupling regime In the strong coupling regime, as in the weak coupling regime, the eigenvalues of the cavity and dot can be found from Eq. (2) with the condition that $g \geq \frac{\kappa}{2}$. In this case the square root becomes imaginary. The cavity and quantum dot cannot be treated separately, but exist in a time dependent superposition state, with photons exchanging energy between the two at a rate of $\approx 2g$. The eigenvalues of this system are

$$\omega_{\pm} = -\frac{(\kappa+\gamma)}{2} \pm i\sqrt{g^2 - \left(\frac{\kappa-\gamma}{2}\right)^2} \quad (7)$$

$$\approx -\frac{(\kappa+\gamma)}{2} \pm ig \quad (8)$$

By improving the fabrication of our PC cavities, we have been able to fabricate cavities with Q's in the range of 10000 to 15000, with the best case of 25,500. In such cavities, we have been able to observe strong coupling. Figure 4 shows a scanning electron microscope (SEM) image of such a cavity with Q=10,500 and the photoluminescence observed from the cavity as a quantum dot is tuned through the cavity resonance via temperature. However, since the dot is strongly coupled to the cavity, the dot line never crosses the cavity line. Instead, when the two are exactly on resonance, we observe the characteristic splitting predicted by Eq. (8). For clarity, we track the quantum dot and cavity peaks at the different temperature points and plot them in Fig. 4 (c).

The polariton splitting is on the order of 0.05nm, which is equal to the field decay rate κ, suggesting that we operate at the onset of strong coupling with $2g/2\pi = 16GHz = \kappa/2\pi$, where a full Rabi oscillation does not occur.

4 Interaction between coherent light and a quantum dot in a PC cavity: experiment The strong interaction between a quantum dot and a cavity in a PC architecture can be used to create logic gates and nodes in a quantum network, based on several quantum information processing schemes [1,2]. These proposals rely on the modification of the cavity transmission due to the presence of a coupled atom or quantum dot. When the quantum dot is coupled to the PC cavity, it can prohibit photons from passing through it. Furthermore, the quantum dot behaves as a saturable absorber at very low powers [10], and, because most photons are radiated into a single mode in PC cavities, it can be used as a Kerr medium for the realization of quantum gates.

4.1 Theory The theory for the transmission function of a cavity containing a well coupled emitter under weak excitation can be found in [9,2], and has been extended to the strong excitation regime in [11,10]. The analytical

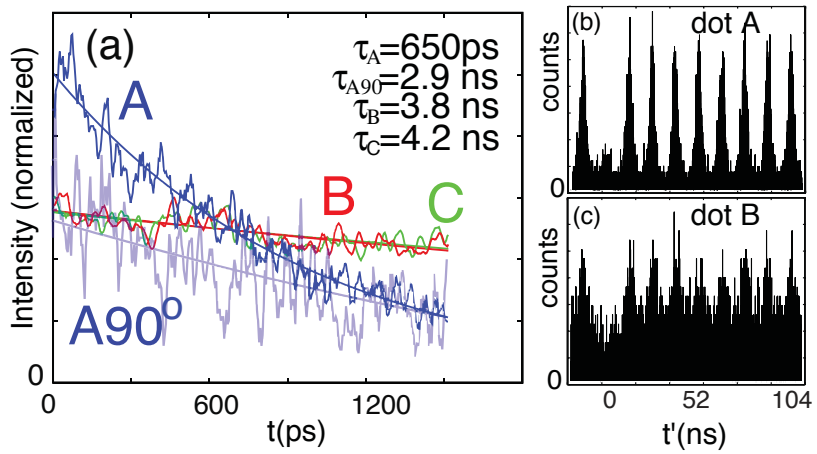

Figure 2 (a) Lifetime measurements on different QDs positioned at various points inside a PC cavity. The normalized intensity for three quantum dots A,B and C coupled to a PC cavity mode is shown as a function of time. The signal from quantum dot A along the polarization orthogonal to the PC cavity is shown along A90°. The emission rates of cavity coupled dots (A) are enhanced, while emission of uncoupled (B,C) and dots orthogonal to the cavity mode (A90°) is suppressed. (b,c) Measurements of the photon autocorrelation function on quantum dots A and B in (a). In both cases, antibunching at $\tau = 0$ indicates that single emitters are probed. The emission rate of quantum dot A is enhanced by the cavity, while that of quantum dot B (c) is suppressed, as can be seed from the width of the autocorrelation peaks in (a,b).

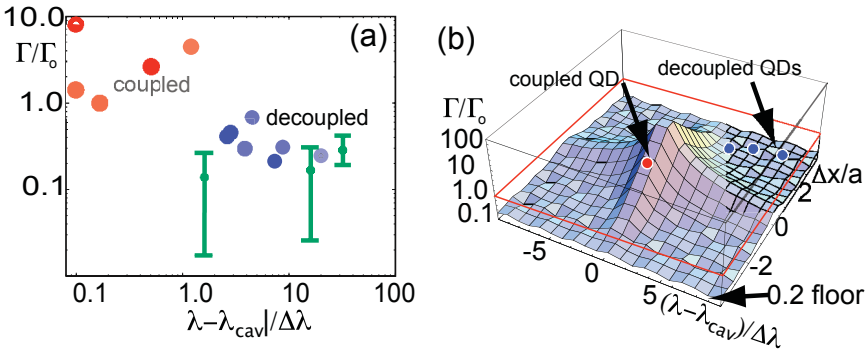

Figure 3 Spontaneous emission rate modification. (a) Experimental (circles) and calculated (bars) data of γ_c/γ of single QD lines vs. spectral detuning (normalized by the cavity linewidth λ_c/Q). Coupling was verified by spectral alignment and polarization matching. (b) Illustration of the predicted spontaneous emission rate modification in the PC as function of normalized spatial and spectral misalignment from the cavity (a is the lattice periodicity). This plot assumes Q = 1000 and polarization matching between the emitter dipole and cavity field. The actual spontaneous emission rate modification varies significantly with exact QD location.

form of the transmission is given by

$$R = \eta \left| \frac{\kappa}{i(\omega_c - \omega) + \kappa + \frac{g^2}{i(\omega_d - \omega) + \gamma}} \right|^2 \qquad (9)$$

A plot of this function is shown in Fig. 5. It can be seen that the quantum dot strongly modifies the transmission property of the PC cavity. In particular, photons falling within the bandwidth given by the QD's modified spontaneous emission rate $\frac{g^2}{\kappa}$ are rejected from the cavity. This effect can be observed in both the weak and strong coupling regimes, with the bandwidth of the modified spectrum increasing with higher coupling and higher Q. In order to probe this effect, we used a narrow-bandwidth (5 MHz) tunable external cavity diode laser (Sacher Laser). However, scanning the laser through the cavity line and normalizing by the input power proved difficult, since the bandwidth of the cavity is quite large when compared to the modehop-free tuning range of the laser.

4.2 Temperature tuning To obtain the best signal to noise in our measurement, we choose to fix the probe laser frequency, and modulate the cavity and dot resonance using our temperature tuning technique, developed in [7]. While this proves to be a useful tool for our experiment, the most important impact of this tuning technique is that it allows us to independently tune multiple PC nodes consisting of dots in cavities into resonance with each other. This bypasses the problem of dot and cavity alignment caused by fabrication imperfections and the large inhomogeneous QD broadening, which have been considered to be the biggest impediment to scaling up to quantum networks based on multiple cavities and dots interacting with each other. Our in-situ technique allows extremely precise spectral tuning of InAs quantum dots by up to 1.8nm and of cavities of up to 0.4 nm (4 cavity linewidths). The tech-

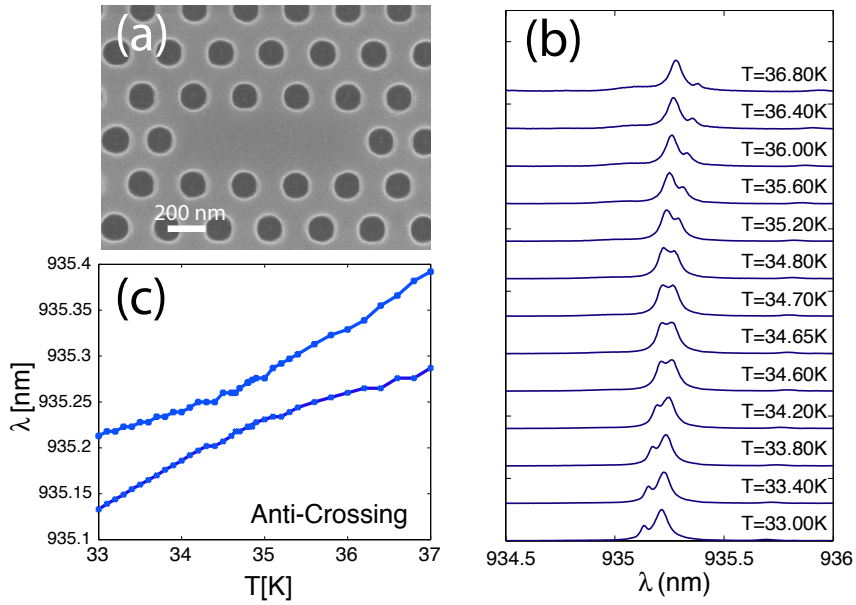

Figure 4 (a) Scanning electron microscope (SEM) image of a PC cavity in which strong coupling is observed. (b) Photoluminescence of a quantum dot strongly coupled to a photonic crystal cavity, for different detunings between the cavity and dot. The dot wavelength is controlled by the temperature of the sample, which is controlled by the cryostat. The cold-cavity Q-factor is around 10500, and the mode volume is $\approx 0.75\,(\lambda/n)^3$. (c) Peak positions of photoluminescence in Panel (b) as a function of temperature. The dot and cavity line never cross, indicating that they behave as predicted for the strong coupling regime.

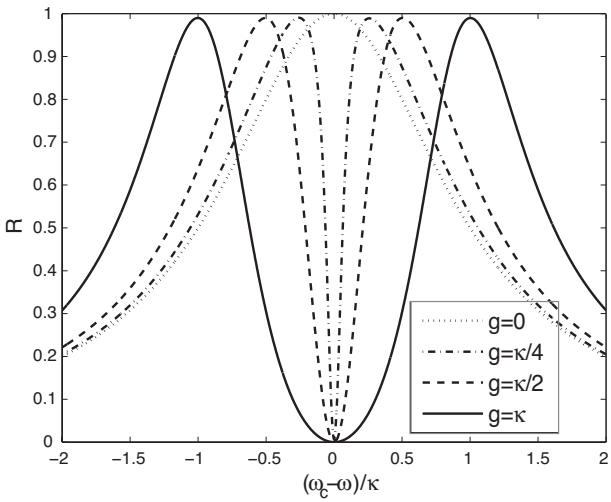

Figure 5 Transmission of a cavity containing a coupled quantum dot on resonance with the cavity mode for several values of the coupling parameter g, as predicted by Eq. (9). When the dot is decoupled from the cavity $g = 0$, the transmission function is a Lorentzian with a linewidth corresponding to the cavity Q. When the dot is coupled, photons cannot pass at the cavity resonance. The bandwidth of the rejection window increases with larger coupling.

nique is crucial for spectrally aligning distinct quantum dots on a photonic crystal chip and forms an essential step toward creating on-chip quantum information processing devices.

To achieve independent on-chip tuning, distinct regions of the chip must be kept at different temperatures. We achieve this by thermally insulating individual cavities from the rest of the sample via trenches, thus overcoming the good thermal conductivity of bulk GaAs. The fabricated tuning structure is shown in Fig. 6. The tuning behavior of the quantum dot and the cavity is shown in Fig. 7. The quantum dot resonance depends quadratically on power, consistent with the bandgap change, while the cavity is sensitive to the refractive index change and tunes at 1/3 to 1/4 the rate of the quantum dot. We further verify that the heating does not perturb the single quantum dot in the PC cavity, and that it still acts as a single photon source, indicating that this technique is compatible with a quantum device. Thus, rather than altering the temperature of the cryostat, we use local heating to tune a quantum dot into strong coupling, similarly to Fig. 4.

4.3 Cavity reflectivity Using the device structure shown in Fig. 6, we measured the reflectivity of a PC cavity with a highly coupled dot. We start with a quantum dot, which exhibits an anticrossing with the cavity mode, as shown in Fig. 8 (a). During the experiment, the probing laser frequency is fixed to lie closely to the point where the temperature tuned quantum dot intersects the cavity reso-

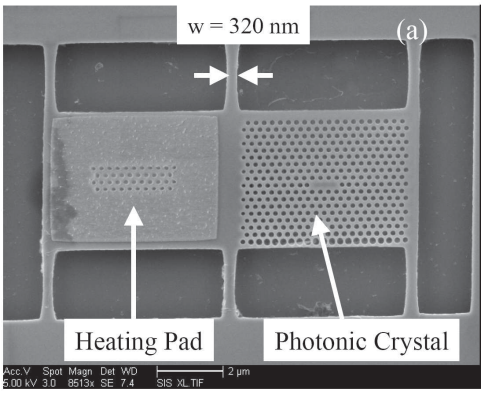

Figure 6 Scanning electron microscope image of the fabricated structure showing the PC cavity, the heating pad and the connection bridges. The temperature of the structure is controlled with a laser diode (960 nm) focused on the heating pad. We use 960 nm in order to prevent excitation of the quantum dots by carrier generation or resonant pumping.

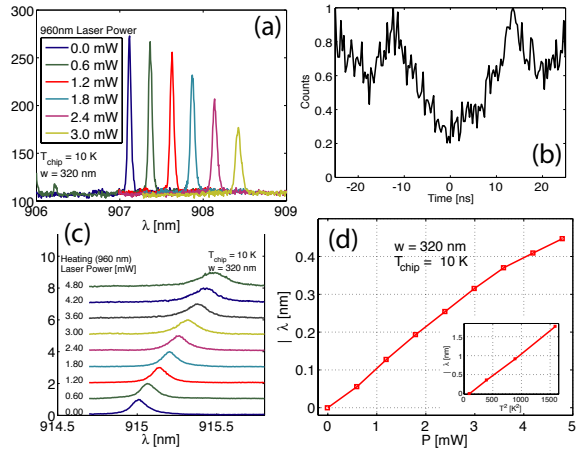

Figure 7 (a) Quantum dot tuning vs. heating pump power. The structure is connected to the substrate by bridges measuring 320 nm in width. The quantum dot emission shifts by 1.4 nm while increasing the heating laser power to 3 mW. Only a small fraction of the heating laser power is absorbed in the metal pad. (b) Autocorrelation measurement showing single photon anti bunching while the QD was detuned by 0.8 nm using the local tuning technique. (c) Detuning of the PC cavity resonance with increasing temperature due to local heating. (d) Dependence of the PC cavity resonance wavelength on the local heating power. The inset shows that the dot wavelength is linear with T^2. The connecting bridges had a width of 320 nm and the cryostat was set to a base temperature of 10 K.

nance. Our temperature tuning technique is then used to tune both, the dot and the cavity through the laser line. Since the dot tunes faster than the cavity, we are able to tune the dot through the anticrossing point, and monitor this with the probe beam. In order to reject the direct laser scatter, we send in a vertically polarized probe beam at 45 degrees to the cavity. The light which is coupled to the cavity is reemitted with a horizontal component. We observe this horizontal component after a polarizing beam cube. Thus we are able to reject a large fraction of the directly scattered light.

The results of the measurement are shown in Fig. 8(b). From the width of the splitting in (a), we obtain a value of $g/2\pi = 8$ GHz$= \kappa/2$. As expected from the theory in Eq. (9), the cavity reflectivity is strongly modified. The observed reflectivity does not drop down directly to zero at the dot resonance. We attribute this discrepancy to experimental noise. In particular, we observed that the temperature of the heating laser fluctuated by 0.7%, which resulted in a fluctuation of the quantum dot on the order of 0.005 nm. We obtain good agreement with the theory, when account for this fluctuation. The coupling efficiency was found to be 2%.

Finally, we explore the nonlinear behavior of this system, by increasing the power of the probing laser. As shown in Fig. 8(c), we observe saturation at power levels which correspond to several photons in the cavity, which indicates one of the largest optical nonlinearities available in the solid state systems. The major advantage of this nonlinearity is that photons are conserved, because they are primarily re-emitted into the cavity mode. While our current coupling efficiency of 2% is quite low, this can be greatly improved when the probe laser is coupled to the cavity via a waveguide, and this nonlinearity can be used for on-chip photon-photon interactions.

5 Conclusion In conclusion, we have presented our recent progress toward the realization of a quantum information processing network on a chip. We have been able to create devices that allow us to explore the weak and strong coupling regimes for InAs quantum dots in PC cavities. We have developed a novel technique for independent frequency tuning of quantum dots and cavities on the same chip, and have applied this technique to a spectroscopic measurement of a single quantum dot in a PC cavity. This measurement has revealed that the presence of the quantum dot can strongly alter the transmission function for the

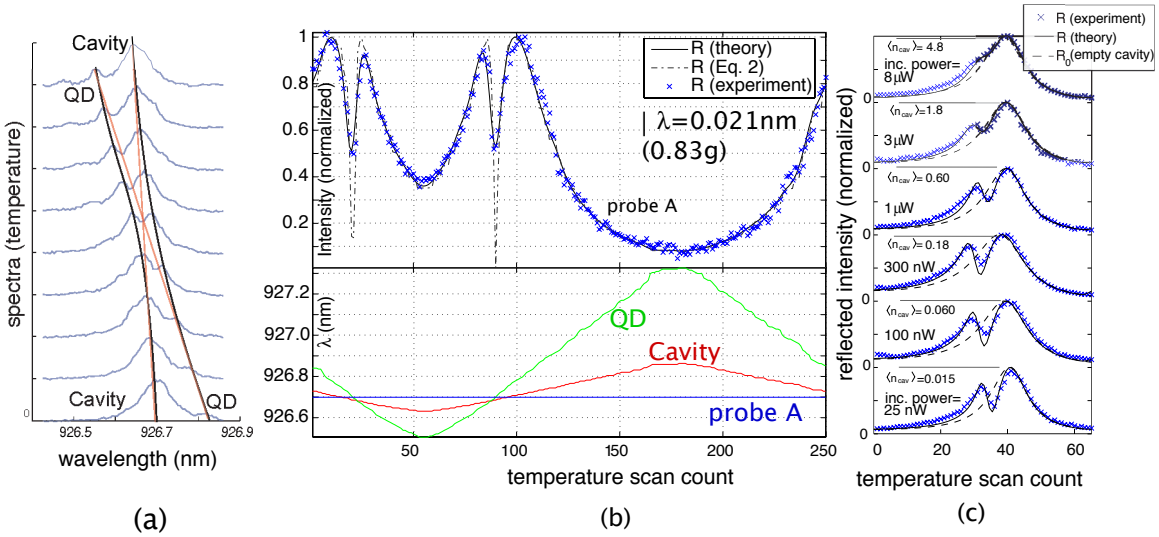

Figure 8 (a) A strongly coupled quantum dot, which exhibits anticrossing with a coupling $g/2\pi = 8$ GHz$= \kappa/2$ is resonantly probed. Spectra at different values of temperature show how the dot traverses the cavity. (b) The probing laser (probe A) frequency is set closely to the point of anticrossing as shown in the bottom panel. The temperature tuning shifts both, the dot (QD) and cavity (Cavity) lines through the probe. The temperature tuning is driven by a triangular wave. In the top panel of (b) we show the amplitude of the reflected beam, which traces out the cavity reflectivity. A fit to the theory (Eq. (9)) with cavity and dot parameters taken from spectral data in (a) matches the experimental data. When we take thermal fluctuations due to heating laser power stability into account in our theory, the fit matches the data very well. In (c) we progressively increase the power of the probe laser. We observe that the dip begins to saturate at powers, which correspond to ≈ 1 photon inside the cavity per cavity lifetime. The powers were measured before the objective lens, while photon numbers are obtained from theoretical fits.

PC cavity, and could serve as a state readout method for a coupled quantum dot. This same effect can be exploited to route quantum information carrying photons on a chip and realize entanglement between nodes in a quantum network. The giant optical nonlinearity will be further explored as a means to realize conditional phase gates and switching. A Kerr nonlinearity such as the one shown in our experiment is attractive for a photon-photon switching device. The architecture of the PC circuit, and the fact that photons are conserved inside the propagation channel due to a high value of β, makes this an ideal system for multiply cascaded nonlinear gates operating on single photons. A similar concept has been realized in atomic physics [12], but due to the macroscopic nature of the experiment, scaling and cascading is difficult. Furthermore, this value of nonlinearity can be used to realize switching at fundamentally lowest power levels given by energies of single photons mediated by a single atom, and may find applications in moderately powered classical information processing devices.

Acknowledgements We thank Nick Stoltz in the Pierre Petroff group at University of California at Santa Barbara for providing us with quantum dot samples used in the work on strong coupling. We thank Bingyang Zhang in the Yoshihisa Yamamoto Group at Stanford University for providing us with samples for work on single photon sources. Financial support was provided by the ONR Young Investigator Award and MURI Center for photonic quantum information systems (ARO/DTO Program). D.E. and I.F. were also supported by the NDSEG fellowship. Work was performed in part at the Stanford Nanofabrication Facility of NNIN supported by the National Science Foundation.

References

[1] L. Duan and H. Kimble, Phys. Rev. Lett. **92**, 127902 (2004).
[2] E. Waks and J. Vučković, Phys. Rev. Lett. **80**, 153601 (2006).
[3] D. Englund, A. Faraon, B. Zhang, Y. Yamamoto, and J. Vučković, Opt. Express **15**, 5550 (2007).
[4] D. Englund, D. Fattal, E. Waks, G. Solomon, B. Zhang, T. Nakaoka, Y. Arakawa, Y. Yamamoto, and J. Vučković, Phys. Rev. Lett. **95**, 013904 (2005).
[5] T. Yoshie, A. Scherer, J. Hendrickson, G. Khitrova, H. M. Gibbs, G. Rupper, C. Ell, O. B. Shchekin, and D. G. Deppe, Nature **432**, 200 (2004).
[6] K. Hennessy, A. Badolato, M. Winger, D. Gerace, M. Atatüre, S. Gulde, S. Falt, E. Hu, and A. Imamoglu, Nature **445**, 896 (2007).
[7] A. Faraon, D. Englund, I. Fushman, N. Stoltz, P. Petroff, and J. Vuckovic, Appl. Phys. Lett. **90**, 213110 (2007).
[8] D. Englund, A. Faraon, I. Fushman, N. Stoltz, P. Petroff, and J. Vuckovic, Nature (2007) (in press) .
[9] H. J. Kimble, in: Cavity Quantum Electrodynamics, edited by P. Berman (Academic Press, San Diego, 1994).
[10] A. Auffves-Garnier, C. Simon, J. Grard, and J. P. Poizat, Phys. Rev. A **75**, 053823 (2007).
[11] R. Thompson, Q. Turchette, O. Carnal, and H. J. Kimble, Phys. Rev. A **57**, 3084 (1998).
[12] Q. Turchette, C. Hood, W. Lange, H. Mabuchi, and H. J. Kimble, Phys. Rev. Lett. **75**, 4710 (1995).